Advances in Environmental Technology 1 (2021) 47-56

Iranian Reasearch Organization for Science and Technology (IROST)

Advances in Environmental Technology

Journal home page: https://aet.irost.ir/

The CO_2 removal of flue gas using hollow fiber membrane contactor: a comprehensive modeling and new perspectives

Masoud Noordokht, S. Majid Abdoli*

Chemical Engineering Faculty, Sahand University of Technology, Sahand New Town, Tabriz, Iran

ARTICLE INFO

Article history:
Received 10 July 2021
Received in revised form
1 Sptember 2021
Accepted 5 September 2021

Keywords:
HFMC
CO_2 capture
Shell and tube
Baffles
Computational fluid dynamics

ABSTRACT

In this study, a novel hollow fiber membrane contactor (HFMC) under a non-wet condition was numerically explored by CFD techniques based on the finite element method to capture CO_2 from the CH_4/CO_2 gas mixture. A new design, such as a shell and tube heat exchanger with baffles, was proposed. The MEA, DEA, and TEA, as different amines solutions, were selected as the liquid solvents. A CO_2-containing gas mixture and amine solution were passed in the shell side and the tube side of the membrane contactor, respectively. The simulation findings indicated a good agreement with the reported experimental data demonstrating that such a model would evaluate the effects of different parameters during the HFMC system. Specifically, the results showed that the baffles' presence improved the separation efficiency due to the increased residence time on the shell side. The results also indicated that the MEA solution had the highest CO_2 absorption. In the new design (shell and tube heat exchanger with baffles), the rising solvent inlet velocity, decreasing gas velocity, and counter-current flow pattern positively affected separation efficiency.

1. Introduction

Today, rising greenhouse gasses pose a massive threat to human life [1]. Carbon dioxide is a significant greenhouse gas emitted by human activities. The industrial activities of the power generation sectors are the primary source of CO_2 [2,3]. Therefore, it is essential to develop a high-efficiency separation system to decrease CO_2 from gas mixtures. The absorption of CO_2 by chemical solvents, such as aqueous amine solutions, as a practical solution has gained the industry's attention. Among the various methods [4-6], HFMC [7,8] is an advanced technology capable of absorbing CO_2 without the issues of the absorption columns such as foaming, entraining, channeling, and flooding [9]. Other significant advantages of this system over conventional column contactors have attracted considerable attention over the recent decades: size reduction, operational flexibility, elevated mass transfer rate, linear scale-

*Corresponding author: Tel: +984133459171
Email address: abdoli@sut.ac.ir
DOI: 10.22104/AET.2021.5060.1371

up, high contact area per unit volume, and integration possibility [10]. Keshavarz et al. investigated the membrane contactor's performance under non-wetting and partially wetted modes [11]. The CO_2 absorption was observed to decrease with increased wetting of the membrane. In gas-liquid contractors, the gas phase on one side and the liquid solvent on the other side are in contact as co-current or counter-current. Saidi et al. studied the effect of MDEA, DEA, and blends on CO_2 capture with mathematical modeling [12]. They concluded that due to DEA's high reactivity with CO_2 compared to others, it is the best in CO_2 capture. Gilassi and Rahmanian modeled a hollow fiber membrane through computational fluid dynamics and compared the efficiency of three different solvents to remove CO_2 [13]. The solvents used included mono-ethanolamine (MEA), di-ethanolamine (DEA), and n-methyl di-ethanolamine (MDEA). Their findings indicated that MEA would absorb more CO_2 than DEA and MDEA. The effect of single solvents such as H_2O, ethylenediamine (EDA), DEA, MEA, piperazine (PZ), and mixed solvents (DEA/PZ) on CO_2 capture was investigated experimentally by Zhang et al. [14]. The results revealed that PZ has the highest absorption efficiency compared to other single solvents, and the efficacy of CO_2 removal for mixed solvents is 20% better than single ones. Talaghat and Bahmani explored the influence of MEA, MDEA, and their combination on CO_2 removal performance with mathematical modeling [15]. They observed that MDEA had a low CO_2 absorption capacity and increased CO_2 capture efficiency by adding MEA to MDEA. Ghobadi et al. worked experimentally with MEA, TEA, and DEA solutions on CO_2 absorption in HFMC [16]. They found that MEA was a better solvent than DEA and TEA. Taghvaie and Heydarinasab investigated numerical simulation for a non-wetting model of operation and counter-current gas and liquid flow [17]. They used potassium threonate (PT), PZ, and MDEA for CO_2 separation from a CO_2/CH_4 mixture and investigated the hollow fiber membrane contactor porosity and module length. Their results showed that the PZ solvent had higher absorption than the others. Additionally, increasing the length and porosity of the module improved CO_2 separation efficiency. Hongxia et al. investigated theoretical modeling of the mass transfer for CO_2 capture in HFMC for non-wetted and partially wet operation modes. They compared 4-diethylamino-2-butanol (DEAB) performance with MEA, DEA, MDEA, and 2-amino-2-methyl-1-propanol (AMP) solvents [18]. They concluded that the non-wetted membrane had higher efficiency than the partially-wetted one, and MEA had higher absorption than the others. Despite extensive studies [19-21] in the explained research field, the challenge remains to determine how the physical design of HFMCs affects CO_2 capture. This study proposes a novel and different design of a HFMC, such as a shell and tube heat exchanger with baffles to capture CO_2 from the CO_2/CH_4 gas mixture. Comprehensive modeling and simulation of the removal of CO_2 are numerically studied using CFD in the HFMC system. Eventually, the effects of liquid and gas velocity, solvent type, and flow pattern are investigated.

2. Modeling procedure

A comprehensive two-dimensional cylindrical model was proposed and used to study the separation performance of CO_2 from a two-component gas mixture (CO_2/CH_4) in an HFMC using amine solutions as solvents. The model was developed for non-wetted conditions. Due to the small size of the CO_2 molecule compared to methane molecules [22], only the CO_2 passes through the membrane. As depicted in Figure 1, there are three sections within the contactor, including the cylindrical tube, membrane, and shell side. The CO_2 and CH_4 pass into this system's shell side, with several baffles, while different solvents are pumped into the tube side. The CO_2 molecules pass through the membrane from the shell side to reach the tube section, react with the amine in the tube area, and leave the system. The specifications and operating conditions of the membrane contactors and the solvents used in this study are summarized in Table 1 and Table 2, respectively.

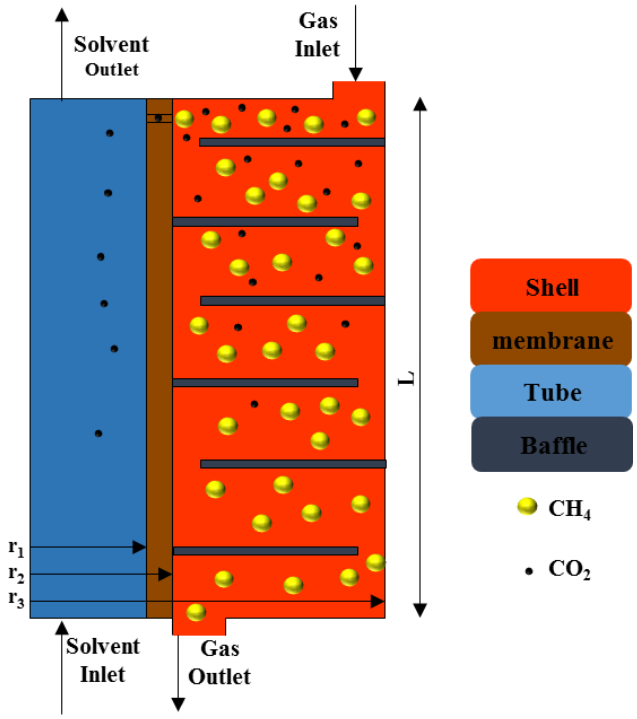

Fig. 1. Schematic of a hollow fiber membrane gas-liquid contactor.

Table 1. Specifications of the membrane contactor and operating conditions [23].

Parameter	Symbol	Value / equation
Diffusion coefficient of CO_2 in shell (m^2/s)	$D_{CO_{2-shell}}$	$2.35\times10^{-6}\, e^{-\frac{2119}{T}}$
Diffusion coefficient of CO_2 in membrane (m^2/s)	$D_{CO_{2-membrane}}$	$D_{CO_{2s}}\varepsilon/\tau$
Inlet gas temperature (°C)	T_g	77
Inlet solvent temperature (°C)	T_s	25
Inlet gas concentration (mol/m^3)	$C_{total-shell}$	1
Inlet CO_2 concentration (mol/m^3)	$C_{CO_2-shell}$	0.1
Membrane Tortuosity (-)	τ	2
Membrane Porosity (-)	ε	0.62
Tube radius (mm)	r_1	1.0
Fiber thickness (mm)	$r_2 - r_1$	0.45
Module radius (cm)	r_3	1.05
Fiber length (cm)	L	24
Baffle height (mm)	B_l	0.18

Table 2. The specifications of solvents used in this study.

Solvent	Symbol	Density (kg/m^3)	Reference
Di-ethanolamine	DEA	1097	[24]
Mono-ethanolamine	MEA	1012	[25]
Tri-ethanolamine	TEA	1124.5	[24]

2.1. Governing equations

The shell side, membrane, and tube side as three sections of the HFMC system are modeled with separately governing equations based on the following assumptions.

- Steady-state and isothermal condition
- Uniform membrane pore distribution
- Axisymmetric approximation
- Henry's law for gas-liquid equilibrium
- Non-wetting operational status
- Ideal gas behavior within the shell.

2.1.1. Shell side

The mass balance equation for each species can be written as Equation (1) to model the mass transport through the HFMC.

$$\frac{\partial C_i}{\partial t} = -D_i \nabla^2 C_i - \nabla . C_i u_z + R_i \quad (1)$$

in which C_i, D_i, and R_i are respectively the concentration, diffusion coefficient, and reaction rate of species i, u_z is the axial velocity, and t is time. Considering Fick's law in a cylindrical coordinate, steady-state condition, and the non-reactive CO_2 transport inside the shell side, Equation (1) becomes Equation (2) [26]:

$$D_{CO2-shell}\left[\frac{\partial^2 C_{CO2-shell}}{\partial r^2} + \frac{1}{r}\frac{\partial C_{CO2-shell}}{\partial r} + \frac{\partial^2 C_{CO2-shell}}{\partial z^2}\right] = u_{z-shell}\frac{\partial C_{CO2-shell}}{\partial z} \quad (2)$$

where $D_{CO2-shell}$, $C_{CO2-shell}$ and $u_{z-shell}$ deote diffusion coefficient, concentration, and axial velocity of CO_2 on the shell side, respectively. The gas stream in the shell section is assumed turbulence flow. $u_{z-shell}$ is the axial velocity in the shell section and can be calculated by Equation (3) [26]:

$$u_{z-shell} = 2\overline{u}_{shell}\left[1-\left(\frac{r_2}{r_3}\right)^2\right] \times \left[\frac{(r/r_3)^2 - (r_2/r_3)^2 + ln(r_2/r)}{3 + (r_2/r_3)^4 - 4(r_2/r_3)^2 + 4\,ln(r_2/r_3)}\right] \quad (3)$$

where $\overline{u}_{shell}$ is the average velocity in the shell side. The shell side boundary conditions are described below:

Z=0 : $\partial C_{CO2-shell}/\partial r = 0$

Z = L : $C_{CO2-shell} = C_{initial}$

r = r_2 : $C_{CO2-shell} = C_{CO2-membrane}$

r = r_3 : $\frac{\partial C_{CO2-shell}}{\partial r} = 0$

2.1.2. Membrane section

The possibility of liquid penetrating the membrane pore is known as membrane wetting, which depends on the membrane's hydrophobic and hydrophilic properties. Membranes are classified as non-wetted, fully-wetted, or partially-wetted based on their wetting modes. In non-wetted mode, the membrane pores are filled with gas, resulting in minimum membrane resistance to mass transfer. In fully-wetted mode, the membrane pores are totally filled with liquid, resulting in the maximum membrane resistance to mass transfer. The liquid penetrates the pores and partially fills the membrane pores in the partially wetted condition. Figure 2 depicts a schematic representation of these three modes. The membrane used in this study is similar to the Kim and Yang polytetrafluoroethylene (PTFE) membrane [23]. They state that this membrane type is non-wetted by aqueous solutions [23]. By considering the non-wetted membrane as diffusion-controlled in a steady-state condition, the mass balance for the transport of CO_2 inside the membrane can be written as Equation (4).

$$\boldsymbol{D_{CO2-membrane}\left[\frac{\partial^2 C_{CO2-membrane}}{\partial r^2} + \frac{1}{r}\frac{\partial C_{CO2-membrane}}{\partial r}\right] = 0} \quad (4)$$

The effective diffusivity coefficient that accounts for the membrane's porosity and tortuosity can be defined as Equation (5) [26]:

$$D_{CO2-membrane} = D_{CO2-shell}\frac{\varepsilon}{\tau} \quad (5)$$

where ε and τ are the porosity and the tortuosity of the membrane, respectively. The boundary conditions at the membrane section are defined as:

r = r_1 : $C_{CO2-membrane} = \frac{C_{CO2-tube}}{m_{CO2}}$

r = r_2 : $C_{CO2-shell} = C_{CO2-membrane}$

where m_{CO2} is the solubility of CO_2 in the solvent, which is obtained from Equation (6) [23].

$$\mathrm{m_{CO2}} = 2 \cdot 82 \times 10^6 \mathrm{e}^{-\frac{2044}{\mathrm{T}}} \quad (6)$$

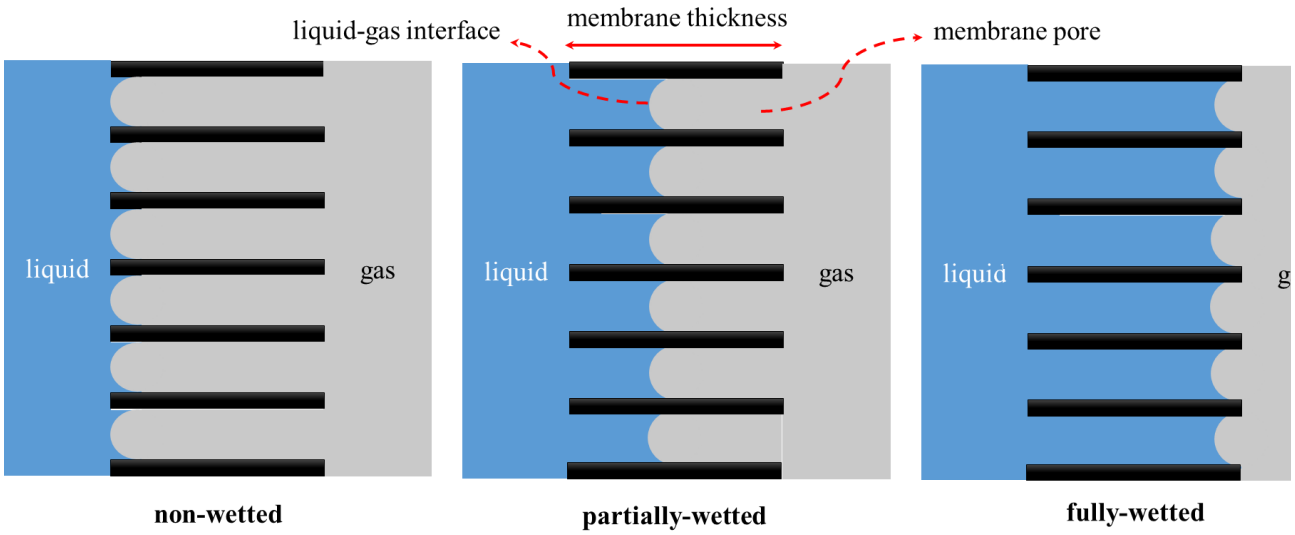

Fig. 2. The schematic of membrane wetting modes.

2.1.3. Tube side

In tube side of HFMC, the steady-state mass balance should be written as Equation (7) for the transport of CO_2 while reacting with solvent, along with the new species generated from the reaction [26]:

$$D_{CO2-tube}\left[\frac{\partial^2 C_{CO2-tube}}{\partial r^2}+\frac{1}{r}\frac{\partial C_{CO2-tube}}{\partial r}+\frac{\partial^2 C_{CO2-tube}}{\partial z^2}\right]+R_i=u_{z-tube}\frac{\partial C_{CO2-tube}}{\partial z} \quad (7)$$

where R_i and $D_{CO2-tube}$ are the reaction rate and diffusion coefficient of CO_2 in the tube, respectively. Table 3 provides the reaction rate and kinetic parameters of CO_2 in different amine solutions. Detailed information on the CO_2-amine reactions can be found in reports by Horng and Li [27]and Liao and Li [28]. u_{z-tube} is the axial velocity in the tube section by assuming laminar flow and can be calculated by Equation (8) [26]:

$$u_{z-tube}=2\overline{u}_{tube}\left[1-\left(\frac{r}{r_1}\right)^2\right] \quad (8)$$

where $\overline{u}_{tube}$ is the average velocity of the solvent in the tube. The boundary conditions are defined as below:

Z = 0 : $C_{CO_2-tube}=0$, $C_{absorbent}=C_{absorbent-in}$

Z = L : $C_{CO_2-tube}=C_{CO_2-absorbed}$

r = 0 : $\frac{\partial C_{CO2-tube}}{\partial r}=0$

r = r_1: $C_{CO2-tube}=C_{CO2-membrane}\times m_{CO2}$, $\frac{\partial C_{absorbent-tube}}{\partial r}=0$

3. Results and discussion

For numerical solution, the Finite Element Method (FEM) was utilized with proper boundary conditions described in the previous section, reaction rate equations with their kinetics, chemical, and physical properties. The simulation parameter values, including viscosity, kinetic parameters, diffusivity, and solubility, related to the absorption of CO_2 were taken from the [24-26], [32-35]. The mesh independence analysis was done to optimize the number and type of mesh in the simulation to demonstrate the gas behavior in three sections (tube, membrane, and shell). Figure 3 depicts the generated mesh in the simulation of CO_2 capture in a membrane contactor. There are 37423 triangular, 3471 edges, and 194 vertex mesh elements with a 1.519×10^{-6} m^2 mesh area.

Table 3. Reaction rate and kinetic parameters of CO_2 in amine solutions.

Solvent	Reaction Rate and Kinetics	Reference
MEA	$CO_2 + OH^- \leftrightarrow HCO_3^{-*}$ $R_1HNH^+COO^- + B \xrightarrow{k_b} R_1R_2NCOO^- + BH^{+**}$ $r_{CO_2-MEA} = \frac{[CO_2][MEA]}{\frac{1}{k_{2,MEA}} + \frac{1}{\frac{k_{2,MEA}\times k_{H_2O}}{k_{-1}}[H_2O] + \frac{k_{2,MEA}\times k_{MEA}}{k_{-1}}[MEA]}}$ $k_{2,MEA}(m^3kmol^{-1}s^{-1}) = 7.973\times10^{12}\, exp\left[-\frac{6243}{T(K)}\right]$ $\frac{k_{2,MEA}\times k_{H_2O}}{k_{-1}}(m^6kmol^{-2}s^{-1}) = 1.1\times10^{6}\, exp\left[-\frac{3472}{T(K)}\right]$ $\frac{k_{2,MEA}\times k_{MEA}}{k_{-1}}(m^6kmol^{-2}s^{-1}) = 1.563\times10^{14}\, exp\left[-\frac{7544}{T(K)}\right]$	[28], [27]
DEA	$CO_2 + OH^- \leftrightarrow HCO_3^{-*}$ $R_1R_2NH^+COO^- + B \xrightarrow{k_b} R_1R_2NCOO^- + BH^{+**}$ $r_{CO_2-DEA} = \frac{[CO_2][DEA]}{\frac{1}{k_{2,DEA}} + \frac{1}{\frac{k_{2,DEA}\times k_{H_2O}}{k_{-1}}[H_2O] + \frac{k_{2,DEA}\times k_{DEA}}{k_{-1}}[DEA]}}$ $k_{2,DEA}(m^3kmol^{-1}s^{-1}) = 1.24\times10^{6}\, exp\left[-\frac{1701}{T(K)}\right]$ $\frac{k_{2,DEA}\times k_{H_2O}}{k_{-1}}(m^6kmol^{-2}s^{-1})(at\ 298K) = 2.20\times10^{-6}$ $\frac{k_{2,DEA}\times k_{DEA}}{k_{-1}}(m^6kmol^{-2}s^{-1}) = 3.18\times10^{7}\, exp\left[-\frac{3040}{T(K)}\right]$	[29] [27]
TEA	$CO_2 + OH^- \leftrightarrow HCO_3^{-*}$ $CO_2 + R_3N + H_2O \leftrightarrow R_3NH^+ + HCO_3^{-**}$ $r_{CO_2-TEA} = k_{2,TEA}[CO_2][TEA] + k_{OH^-}[CO_2][OH^-]$ $k_{2,TEA}(m^3kmol^{-1}s^{-1}) = 0.5315\times10^{7}\, exp\left[-\frac{4304}{T(K)}\right]$	[30], [27]

*Because of the negligible contribution, the CO_2 reaction with H_2O is usually ignored in the overall reaction rate [31].
** R_1, R_2, R_3 are alkyl groups for primary, secondary, and tertiary amines, respectively.

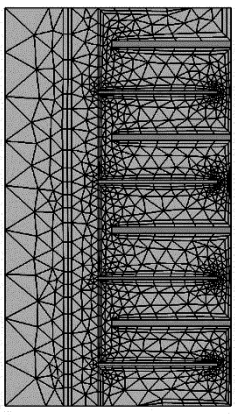

Fig. 3. The mesh geometry used in HFMC system in the simulation of CO_2 separation.

3.1. Validation

The simulation findings for the separation of CO_2 from CH_4 using the HFMC were compared with Kim and Yang's experimental data [23] to verify the two-dimensional proposed model. The CO_2 removal efficiency (η) can be determined as Equation (9).

$$\eta = \frac{C_i - C_o}{C_i} \times 100 \quad (9)$$

where C_i and C_o are the average concentration of CO_2 at the inlet and outlet of membrane contactor, respectively. The CO_2 removal performance in HFMC for different values of liquid flow is given in Figure 4. As shown, rising liquid flow on the tube side of the HFMC improves the membrane's removal efficiency of CO_2. In other words, a high solvent flow rate can remove a significant volume of CO_2 due to the high concentration gradient. It is also seen in Figure 4 that the model predictions are in good agreement with the reported experimental results for various liquid flow values.

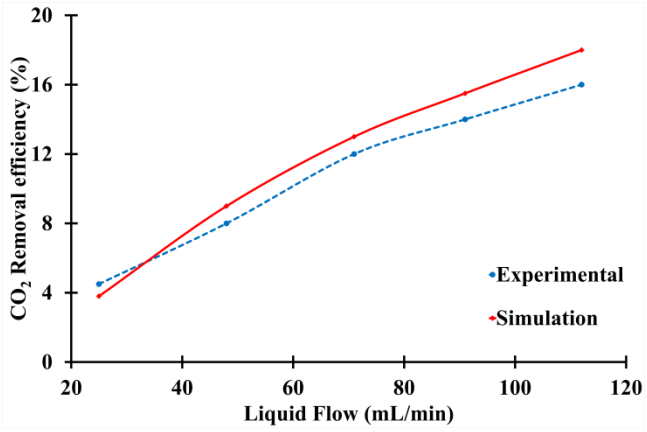

Fig. 4. A comparison of the CO_2 removal efficiency between the simulation and experiment data over various liquid flow.

3.2. New design suggestion

A new design was suggested following the simulation validation conducted for the HFMC system, and CO_2 absorption performance was compared with the old design. Unlike the old design, multiple baffles were situated on the system's shell side in the proposed design. The concentration profiles of CO_2 in HFMC in two different designs and the CO_2 removal efficiency of both are shown in Figures 5 and 6, respectively. As can be seen, in the new design, due to more residence time on the shell side, the CO_2 capture quantity is greater than the old one. It also can be observed, in the same lengths of the two designs, that the concentration of CO_2 in the old design did not exceed zero. In contrast, in the new design, the concentration reached almost zero in the middle of the system, indicating the new design's high efficiency. In other words, more CO_2 can be separated by adding baffle to the old design.

3.3. Effect of solvent velocity and type

A variation in solvent velocity on the tube side changes the concentration of CO_2 at the liquid interface, which creates a higher gradient of concentration. Figure 7 demonstrates CO_2 separation efficiency with different solvent velocities within the range of 0.02 to 0.1 m/s. The CO_2 capture percentage has an ascendant pattern for all solvents (MEA, DEA, and TEA) compared to the rising liquid rate. Increasing the amount of fresh solvent reduces the mass transfer boundary layer's thickness on the tube side. As the resistance decreases, the gas diffusion improves and enhances the average CO_2 concentration absorbed. It can also be seen that the CO_2 removal efficiency of the MEA solvent is high. Three groups of amine solvents are classified into primary, secondary, and tertiary. The amines form carbonates when they react with carbon dioxide. MEA has a faster CO_2 reaction rate because it has two N-H bonds necessary for the carbonate ion to be formed with CO_2, allowing absorption to occur in a shorter column. Whereas TEA reacts slowly with CO_2 due to the lack of the N-H bond required to form the carbonate ion with CO_2. In sum, the adsorption capacity of MEA as the first type of amine is higher than DEA (secondary amine) and TEA (tertiary amine) due to more reactivity with CO_2 relative to the others. Many studies have reached the same conclusion [36,37].

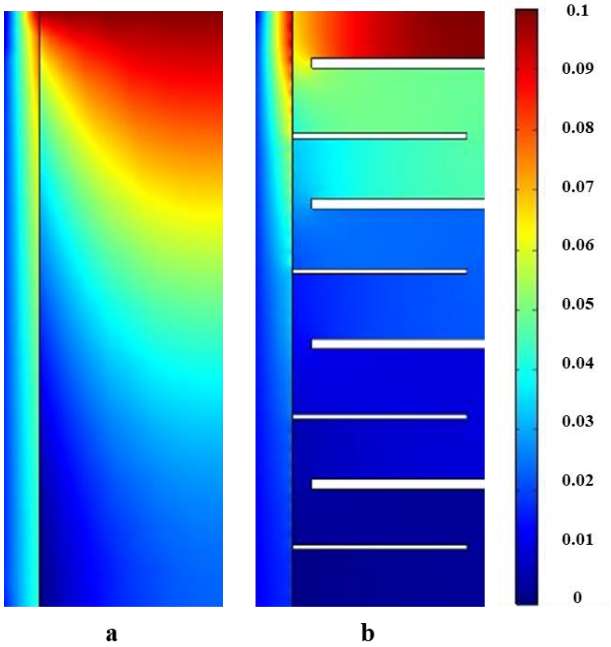

Fig. 5. Concentration profile of CO_2 in HFMC, a) Old Design, b) New Design (Amine mole fraction: 0.3, U_g: 0.01 m/s, U_l: 0.02 m/s, T: 25 °C, solvent: MEA).

3.4. Effect of gas velocity

The efficiency of CO_2 removal heavily depends on the reaction between the solvent and the gas. Figure 8 depicts the CO_2 capture performance variation by gas velocity within the range of 0.0001 to 0.01 m/s. As the gas velocity on the shell side increases, the removal percentage is observed to decrease. The gas's residence time in the shell

reduces as the gas velocity grows. As a result, less gas reaches the tube side through the membrane, and less reaction occurs. As discussed previously, the CO_2 capture percentages for the MEA, DEA, and TEA solvents are reduced, respectively. It is preferable to reduce the gas velocity to improve the performance of the system. It is clear that the gas velocity can be decreased to some extent due to the system pressure drop. In addition, as the gas velocity decreases, the system's ability to purify more gas suffers. As a result, the capacity of the HFMC system is diminished. To overcome this issue, it is recommended that the baffles mentioned earlier be used to maintain the system's capacity at an optimal level.

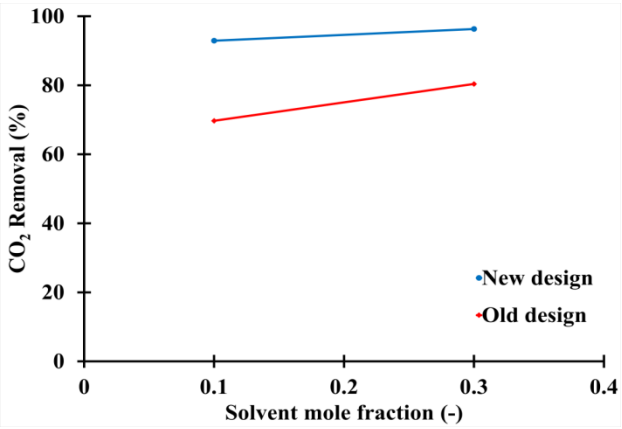

Fig. 6. CO_2 removal efficiency of both new and old designs (U_g: 0.01m/s, U_l: 0.02 m/s, T: 25 °C, solvent: MEA).

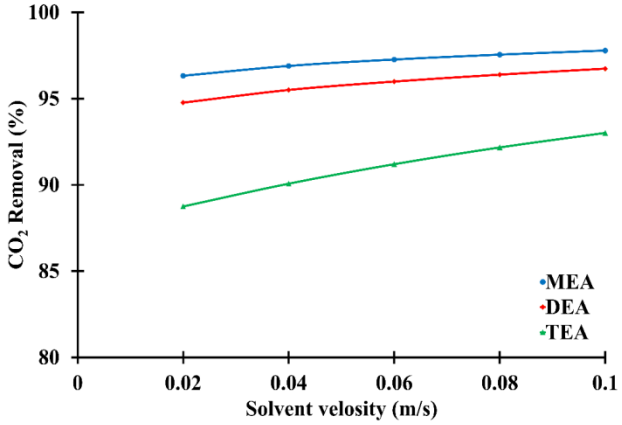

Fig. 7. Variation of solvent velocity on CO_2 removal efficiency in various solvents designs (Amine mole fraction: 0.3, U_g: 0.001 m/s, T: 25 °C).

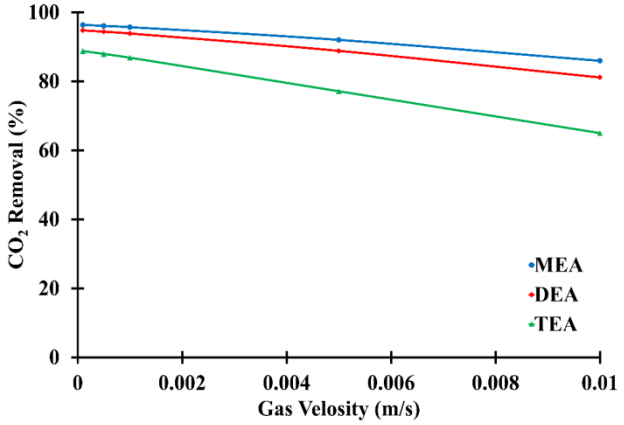

Fig. 9. Variation of solvent velocity on CO_2 removal efficiency in various flow patterns designs (Amine mole fraction: 0.3, U_g: 0.001 m/s, T: 25 °C, solvent: MEA).

4. Conclusions

Understanding the significant parameters and predicting the hollow fiber membrane contactor performance is essential to improve CO_2 capture efficiency. In the current study, the CO_2 absorption process in an HFMC system has been numerically formulated. The computational fluid dynamics technique based on the finite element method was employed for CO_2 mass transfer. The accuracy of the developed model was demonstrated by the comparisons between modeling results and experimental data. The model was used to test the effect of many essential factors after validation with the experimental observation on CO_2 removal performance, including (1) a novel and different design like shell and tube heat exchanger with baffles, (2) solvent type, (3) solvent velocity, (4) gas velocity, and (5) flow pattern. Specifically, the findings revealed that the presence of the baffles increased the efficiency of separation due to the improved residence time on the shell side. The results also indicated that the MEA and DEA solutions, as primary and secondary amines, had the best absorption of CO_2 relative to the other two. It could also be understood that gas velocity negatively influenced CO_2 removal performance, whereas solvent inlet velocity and counter-current flow patterns had positive effects.

References

[1] Naz, R., Shah, M., Ullah, A., Alam, I. and Khan, Y. (2020) An assessment of effects of climate change on human lives in context of local

response to agricultural production in district buner. *Sarhad journal of agriculture*, *36*, 110–9.

[2] Desideri, U. and Paolucci, A. (1999) Performance modelling of a carbon dioxide removal system for power plants. *Energy conversion and management*, *40*, 1899–915.

[3] Akhoondi, A., Osman, A.I. and Alizadeh Eslami, A. (2021) Direct catalytic production of dimethyl ether from CO and CO_2: A review. *Synthesis and sintering*, *1*, 105–25.

[4] Liu, S., Liu, L.-T., Sun, L.-X., Zhou, Y.-L. and Xu, F. (2018) Improved CO_2 capture and separation performances of a Cr-based metal–organic framework induced by post-synthesis modification of amine groups. *Polyhedron*, *156*, 195–9.

[5] Zohdi, S., Anbia, M. and Salehi, S. (2019) Improved CO_2 adsorption capacity and CO_2/CH_4 and CO_2/N_2 selectivity in novel hollow silica particles by modification with multi-walled carbon nanotubes containing amine groups. *Polyhedron*, *166*, 175–85.

[6] Abid, H.R., Rada, Z.H., Liu, L., Wang, S. and Liu, S. (2021) Striking CO_2 capture and CO2/N2 separation by Mn/Al bimetallic MIL-53. *Polyhedron, 193*, 114898.

[7] Gabelman, A. and Hwang, S.T. (1999) Hollow fiber membrane contactors. *Journal of membrane science*, *159*, 61–106.

[8] Mansourizadeh, A. and Ismail, A.F. (2009) Hollow fiber gas-liquid membrane contactors for acid gas capture: A review. *Journal of hazardous materials*, *171*, 38–53.

[9] Sohrabi, M.R., Marjani, A., Moradi, S., Davallo, M. and Shirazian, S. (2011) Mathematical modeling and numerical simulation of CO_2 transport through hollow-fiber membranes. *Applied mathematical modelling*, Elsevier Inc. *35*, 174–88.

[10] Shirazian, S., Rezakazemi, M., Marjani, A. and Rafivahid, M.S. (2012) Development of a mass transfer model for simulation of sulfur dioxide removal in ceramic membrane contactors. *Asia-Pacific journal of chemical engineering*, *7*, 828–34.

[11] Keshavarz, P., Fathikalajahi, J. and Ayatollahi, S. (2008) Mathematical modeling of the simultaneous absorption of carbon dioxide and hydrogen sulfide in a hollow fiber membrane contactor. *Separation and purification technology*, *63*, 145–55.

[12] Saidi, M., Heidarinejad, S., Rahimpour, H.R., Talaghat, M.R. and Rahimpour, M.R. (2014) Mathematical modeling of carbon dioxide removal using amine-promoted hot potassium carbonate in a hollow fiber membrane contactor. *Journal of natural gas science and engineering*, Elsevier B.V, *18*, 274–85.

[13] Gilassi, S. and Rahmanian, N. (2016) CFD modelling of a hollow fibre membrane for CO_2 Removal by aqueous amine solutions of MEA, DEA and MDEA. *International journal of chemical reactor engineering*, 14, 53–61.

[14] Zhang, Z., Yan, Y., Wang, J., Zhang, L., Chen, Y. and Ju, S. (2015) Analysis of CO2 capture from power-plant flue gas using the membrane gas absorption (MGA) method. *American society of mechanical engineers, power Division (Publication) POWER*, p. 1–8.

[15] Talaghat, M.R. and Bahmani, A.R. (2017) Mathematical modeling of carbon dioxide removal from the CO_2/CH_4 gas mixture using amines and blend of amines in polypropylene: A comparison between hollow fiber membrane contactor and other membranes. *Journal of petroleum science and technology*, *7*, 41–53.

[16] Ghobadi, J., Ramirez, D., Jerman, R., Crane, M. and Khoramfar, S. (2018) CO2 separation performance of different diameter polytetrafluoroethylene hollow fiber membranes using gas-liquid membrane contacting system. *Journal of membrane science*, *549*, 75–83.

[17] Nakhjiri, A.T. and Heydarinasab, A. (2020) CFD analysis of CO_2 sequestration applying different absorbents inside the microporous PVDF hollow fiber membrane contactor. *Periodica polytechnica chemical engineering*, *64*, 135–45.

[18] Cao, F., Gao, H., Ling, H., Huang, Y. and Liang, Z. (2020) Theoretical modeling of the mass transfer performance of CO_2 absorption into DEAB solution in hollow fiber membrane contactor. *Journal of membrane science*, *593*, 117439.

[19] Razavi, R., Bemani, A., Baghban, A. and Mohammadi, A.H. (2020) Modeling of CO2 absorption capabilities of amino acid solutions

using a computational scheme. *Environmental progress and sustainable energy*, *39(6), e13430*.

[20] Rohani, R., Yusoff, I.I., Amran, N.F.A., Naim, R. and Takriff, M.S. (2021) Comparison of separation performance of absorption column and membrane contactor system for biohydrogen upgraded from palm oil mill effluent fermentation. *Environmental progress and sustainable energy*, *40(3), e13573*.

[21] Chaalal, O., Hossain, M. A two-step process for removal of carbon dioxide and production of desalinated water using ammoniated saline water. *Environmental progress and sustainable energy*, *35*(1).

[22] Kesting, R.E. and Fritzsche, A.K. (1993) Polymeric gas separation membrane. Wiley-interscience publication, New York.

[23] Kim, Y.S. and Yang, S.M. (2000) Absorption of carbon dioxide through hollow fiber membranes using various aqueous absorbents. *Separation and purification technology*, *21*, 101–9

[24] Concepción, E.I., Gómez-Hernández, Á., Martín, M.C. and Segovia, J.J. (2017) Density and viscosity measurements of aqueous amines at high pressures: DEA-water, DMAE-water and TEA-water mixtures. *Journal of chemical thermodynamics*, *112*, 227–39.

[25] Sobrino, M., Concepción, E.I., Gómez-Hernández, Á., Martín, M.C. and Segovia, J.J. (2016) Viscosity and density measurements of aqueous amines at high pressures: MDEA-water and MEA-water mixtures for CO_2 capture. *Journal of chemical thermodynamics*, *98*, 231–41.

[26] Zhang, Z., Yan, Y., Chen, Y. and Zhang, L. (2014) Investigation of CO_2 absorption in methyldiethanolamine and 2-(1-piperazinyl)-ethylamine using hollow fiber membrane contactors: Part C. Effect of operating variables. *Journal of natural gas science and engineering, 20*, 58–66.

[27] Horng, S.-Y. and Li, M.H. (2002) Kinetics of absorption of carbon dioxide into aqueous solutions of monoethanolamine + triethanolamine. *Industrial and engineering chemistry research*, *41*, 257–66.

[28] Liao, C.H. and Li, M.H. (2002) Kinetics ofabsorption ofcarbon dioxide into aqueous solutions ofmonoethanolamine +N-methyldiethanolamine. *Separation and purification technology*, *68*, 422–7.

[29] Rinker, E., Ashour, S. and Sandall, O. (1996) Kinetics and modeling of carbon dioxide absorption into aqueous solutions of diethanolamine. *Chemical engineering science*, *35*, 1107–14.

[30] Rangwala, H.A., Morrell, B.R., Mather, A.E. and Otto, F.D. (2009) Absorption of co2 into aqueous tertiary amine/mea solutions. *The Canadian journal of chemical engineering*, *70*, 482–90.

[31] Ko, J.J. and Li, M.H. (2000) Kinetics of absorption of carbon dioxide into solutions of N-methyldiethanolamine+water. *Chemical engineering science*, *55*, 161–75.

[32] Caplow, M. (1968) Kinetics of Carbamate Formation and Breakdown. *Journal of the American chemical society*, *90*, 6795–803.

[33] Danckwerts, P. V. (1979) The reaction of CO_2 with ethanolamines. *Chemical engineering science*, *34*, 443–6.

[34] Barth, D., Tondre, C. and Delpuech, J.J. (1984) Kinetics and mechanisms of the reactions of carbon dioxide with alkanolamines: a discussion concerning the cases of MDEA and DEA. *Chemical engineering science*, *39*, 1753–7.

[35] Alvarez-Fuster, C., Midoux, N., Laurent, A., Charpentier, J. C. (1980). Chemical kinetics of the reaction of carbon dioxide with amines in pseudo m-nth order conditions in aqueous and organic solutions. *Chemical engineering science*, *35*(8), 1717-1723.

[36] Aroonwilas, A., Veawab, A. (2004). Characterization and comparison of the CO_2 absorption performance into single and blended alkanolamines in a packed column. *Industrial and engineering chemistry research*, *43*(9), 2228-2237.

[37] Ramachandran, N., Aboudheir, A., Idem, R., Tontiwachwuthikul, P. (2006). Kinetics of the absorption of CO2 into mixed aqueous loaded solutions of monoethanolamine and methyldiethanolamine. *Industrial and engineering chemistry research*, *45*(8), 2608-2616.